

Chapter 4

Regulating Primary Progenitor Cells Response Through Bioengineered Platforms

4.1 Introduction

The use of functional materials for regenerative medicine has been extensively discussed in the literature and it is summarised in chapter 2. However, the role of such materials in controlling the cellular function of stem/progenitor cells still is not well understood. Particularly, using these materials for growing primary progenitor cells and further investigating the role of different physicochemical parameters on cell-material interactions is a need at the current time. In this, the choice of hepatic progenitor cells could be exciting both in terms of enhancing the knowledge in the field as well as finding its clinical usability in diabetic management by differentiating these cells into insulin-producing cells. Earlier studies have explored the possibility of the therapeutic use of insulin-producing cells as one of the promising technologies in managing uncontrolled diabetes [188-199]. Some of the past studies explored the use of bone marrow-derived stem cells (due to their trans-differentiation capacity into functional insulin-producing cells (InPCs) [188-191]. These studies were very limited to the amount of insulin secreted by these cells, which was insufficient to reverse the hyperglycemia in diabetic animal models [192,193].

Another choice of cells that have been explored was embryonic stem cells (ESCs). These have been successfully converted into insulin-producing pancreatic cells to control hyperglycemia in diabetic models [194-197]. Remarkable success has been achieved with these cells towards trans-differentiated InPCs from ESCs that have the capability for producing a relatively higher yield of insulin. Still, it possesses the potential to transform into tumorigenic [198] and post-transplantation requires immunological protection [199]. Recent

studies show that the use of human hepatic progenitor cells (hHPCs) holds the potential to generate insulin-producing cells and these are non-tumorigenic in nature and passes very less immunogenicity [200,201]. Hence, the use of hHPCs could be an alternative choice of cells for generating insulin-producing cells (InPCs) to control hyperglycemia [202-205]. However, in the past, the utility of such cell therapy is limited due to the lack of appropriate platforms which provide better cellular adhesion, survival, and functions. Thus the earlier attempts of hHPCs have failed due to insufficient insulin production [202,203] and short-term cells survival and function [206-208], which remains a major challenge.

Hence, appropriate extrinsic stimulation is required to enhance the trans-differentiation ability of hHPCs into InPCs which can be achieved by using functional materials that pass such properties. However, very little attention has been paid towards the use of active biomaterials, which can support/enhance the differentiation of hHPCs. Here, the use of external stimuli to human fetal liver-derived EpCAM+ve cells (enriched hHPCs) by nanostructured TiO₂ on conducting (CS) and non-conducting (NCS) substrates, as described in Chapter 2, is used for studying the effect on effective differentiation of hHPCs into InPCs. As discussed in chapter 2, the choice of such substrates is to achieve dynamic charge compensation for hHPCs/InPCs while interacting with TiO₂ during differentiation process. It is expected that the strategy effectively generates a large number of glucose-responsive InPCs on CS without the use of transgene or genetic manipulation. Further, it is expected that the adopted strategy will enable to achieve the functional response of InPCs similar to the key features of bona fide human β -cells by showing co-expression of various key β -cell markers and finally able to produce a higher amount of insulin as compared to earlier reported strategies.

4.2 Experimental procedures, chemicals and reagents

All chemicals were from Sigma-Aldrich (St. Louis, MO) and cell culture reagents obtained from Life Technologies (Grand Island, NY). EasySep™ human EpCAM positive selection kit (Cat: 18356, from Stem Cell Technologies, Canada) and antibodies (FITC-conjugated anti-human EpCAM (Cat: 347197, clone: EBA-1, BD Biosciences, USA), Nkx-6.1-PE (Cat: AA 284-314, Antibodies-online Inc., GA, USA), phycoerythrin (PE) conjugated-anti human Pdx-1 (cat: C2419P, clone: 267712, R&D Systems Inc., USA), C-peptide-FITC (Cat: 4593S, Cell Signaling Technology) and insulin antibody (Cat: ab181547, clone: EPR17359, BioLegend Inc., USA) and human Insulin ELISA kit (Cat: RAB032, Sigma) were used. All other chemicals used were of analytical grade. Conducting substrates (ITO coated glass, Macwin India, Delhi) and non-conducting substrates (simple microscopic plain glass slides) were used in this study. These experiments were performed in the laboratory of Dr. Aleem A Khan at Decaan Medical College, Hyderabad [205]. Details about the preparation of a bioengineering platform for achieving the growth of 3D-TiO₂ Nanostructures on CS and NCS has been described in chapter 2. 3D-TiO₂ nanostructured sheets on conducting (CS) and non-conducting (NCS) substrates were prepared using titanium isopropoxide solution in 50% diluted hydrochloric acid (HCl, 37 wt%).

4.3 Cells isolation and immunomagnetic enrichment

Human fetal liver cells were isolated using a two-step collagenase digestion method as previously reported [203]. The liver was harvested after in-situ perfusion with normal saline. Liver tissue was further subjected to two-step collagenase (0.3 %) digestion at 37°C for 30-60 min and filtered through a 40 µm cell strainer to obtain a single cell suspension. Enrichment of human hepatic progenitor cells (hHPCs) was carried out by

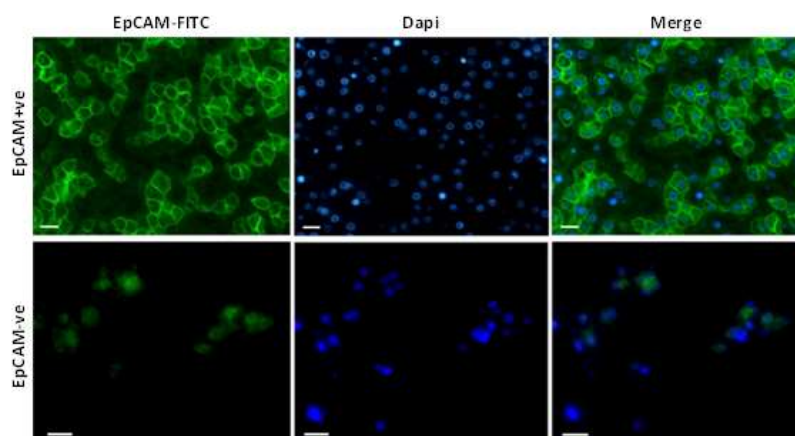


Figure 4.1: Immunofluorescence staining of EpCAM+ve and EpCAM-ve enriched human fetal liver cells stained with anti-human EpCAM-FITC antibodies. Scale bar 20 μ m.

Magnetic Activated Cell Sorting (MACS) using human-directed anti-EpCAM magnetic beads as per the manufacturer's instructions (MiltenyBiotec, Germany). Magnetically sorted EpCAM+ve and EpCAM-ve enriched cells were washed 2-3 times with Hanks buffer after centrifugation at 1000 rpm at 4°C to remove biodegradable microbeads and stained with EpCAM-FITC antibody to identify the percentage of hHPCs (EpCAM+ve enriched) in each population by using immunocytochemical and flow cytometry analysis. EpCAM+ve hHPCs were sorted immunomagnetically from a heterogenous mixture of liver cells derived from human fetal tissues using epithelial cell adhesion molecules (EpCAM) as an eminent HPCs marker. The cells were stained with EpCAM-FITC antibodies, and **Figure 4.1** shows a microscopic fluorescence image of these stained cells. The study was performed per the details reported in our manuscript [120] in which spontaneously aborted human fetuses (gestation age: 12 weeks, gender: male, n=2) were collected after signing informed consent forms from the donor parents. Immunofluorescence images were captured using a fluorescence microscope (Carl Zeiss, Germany) to determine the immune-enriched EpCAM+ve and EpCAM-ve (Germany) and the immune enriched EpCAM+ve and EpCAM-

ve cell fractions. Before staining, cells were fixed in 4% paraformaldehyde (PFA) overnight at 4°C. Following the incubation, cells were treated with bovine serum albumin (1% BSA) solution to block the non-specific binding. Following to blocking step, cells were washed twice with 1X phosphate buffer saline (PBS) and further incubated with EpCAM antibody (1:200 dilution) conjugated with FITC to stain the cell surface.

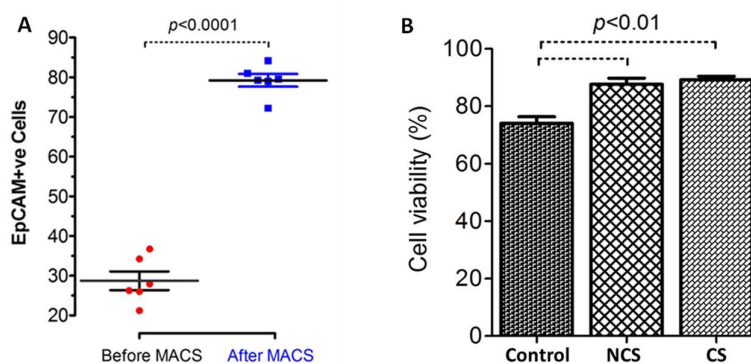


Figure 4.2: (A) Percentage of EpCAM+ve enriched cells before and after immunomagnetic shorting. (B) The percentage survival of hHPCs was much higher (>90%) on NCS and CS supported 3D- nanostructured TiO₂

After staining, cells were washed three times with 1X PBS and mounted with DAPI (4',6-Diamidino-2-Phenylindole, Dihydrochloride) mounting solution on microscopy slides. For flow cytometry analysis, EpCAM stained cells were washed three times, resuspended in 1X PBS. For proper background setting, unstained and IgG controls were run before the sample.

Figure 4.2 shows the relative enrichment of hHPCs before and after immunomagnetic shorting and their viability on three different types of substrates. The viability of these EpCAM+ve enumerated cells (described as hHPCs) showed enhanced cell viability for using TiO₂ surface coated on both CS and NCS. Cell viability was determined by using standard

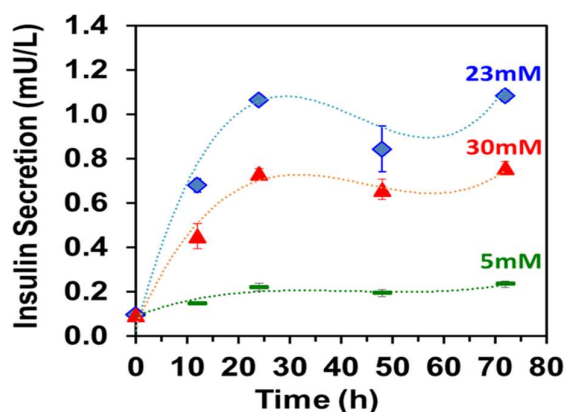


Figure 4.3: Effect of glucose stimulation at three concentrations (5mM, 23 mM, and 30 mM) on hHPCs towards insulin secretion at various time points.

trypan blue and MTT (3-[4,5-dimethylthiazol-2-yl]-2,5-diphenyl tetrazolium bromide) cell viability assays. Tetrazolium reduction assay was performed to estimate the percentage viable cells after 24 hrs of in-vitro culture on collagen-coated cover slips (Corning), 3D-nanostructured TiO₂ on both CS and NCS. 4×10^3 cells were cultured on the above three different types of substrates for 24h in serum-free medium at 37°C and 5% CO₂ atmosphere. 1 mg/mL, MTT (Himedia) was added in each sample, including controls and resultant purple formazan crystals were solubilized with acidified isopropanol (minimum assay (by GC): 99%, Fisher Scientific). Two cohort experiments were performed by including triplicates in experimental groups. Reduction in tetrazolium was estimated as proportional to the cell viability.

4.4 Hyperglycemic stimulation to hHPCs

Glucose-stimulated differentiation of hHPCs into InPCs was performed and the results are shown in **Figure 4.3**. Initially, one million hHPCs were seeded on collagen-coated coverslips in low glucose proliferation medium and allowed to adhere for 4 h. Non-adherent cells were

removed and 50% low glucose medium was replenished. The cells were allowed to grow for 24-48 h and then starved overnight in a serum-free medium containing 0.5 % BSA and 3.0 mM glucose (Sigma). After starvation, the culture medium was replaced with the proliferation medium containing three different concentrations of glucose (5 mM, 23 mM and 30 mM). At each glucose concentration, cells were sequentially incubated for 12 h, 24 h, 48 h and 72 h. After each incubation time at each concentration, the supernatants were collected and insulin was quantified using human insulin ELISA kit (Sigma) with measurement by a DU® 700 Series UV/Vis Spectrophotometers (Beckman Coulter, California, USA) at 450 nm. Serum-free culture medium containing 0.5 % BSA was used as medium control for insulin estimation. Further, to assess the *in-vitro* effect of TiO₂ nanostructures supported with CS and NCS for insulin production, the effect of incubation time (1 day, 3 day and 7 day for one million cells) and cell number (three, six, and nine million cells for 24h) were performed for 23 mM glucose stimulation in culture medium.

A key functional characteristic of β -cells is to produce insulin in response to high glucose stimulus by activating calcium signaling. Hence, the study was performed to monitor calcium ion (Ca²⁺) influx in the hHPCs receiving 5 mM and 23 mM glucose stimulation for 24 h to confirm the physiology of glucose-stimulated hHPCs *in vitro* by staining with Fluo-4AM, a calcium indicator fluorescent dye. Thus, to confirm the *in vitro* functionality of hHPCs during hyperglycemic challenge, we monitored insulin exocytosis by intracellular Ca⁺⁺ signaling with Fluo-4AM (Incell Technologies) immunofluorescence staining. To conduct this experiment, following differentiation protocol on collagen-coated coverslips was performed. Cells were additionally incubated with 50 μ m of Ca⁺⁺ probe (Fluo-4AM-FITC antibody) with Krb buffer containing 5 mM and 23 mM glucose for 45 min in CO₂ incubator. Cells were washed twice with Krb buffer (without glucose) and incubated at 37° C for 15 min. After

hyperglycemic challenge, cells were incubated with Krb buffer containing 30 mM KCl for depolarization challenge. The fluorescence microscopy was performed to measure the calcium flux in glucose-induced cells after binding of Fluo-4AM with Ca^{++} . The fluorescence microscopy results confirmed calcium influx in the glucose induced cells that showed green fluorescence due to binding of Fluo-4AM with Ca^{++} (**Figure 4.4**).

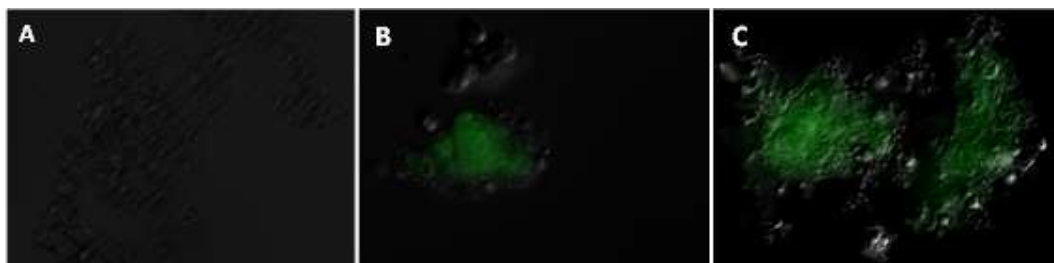


Figure 4.4: Immunofluorescence microscopic observation of calcium flux (after staining with Fluo-4 AM) in hHPCs without glucose stimulation (A), at 5 mM glucose stimulation (B) and 23mM glucose stimulation (C) after 24 h. 23 mM glucose challenge showed highest glucose sensing by hHPCs measured with the amount of green fluorescence. Images are acquired at 20X magnification.

This is important because insulin secretion in β -cells is regulated through calcium signaling which is specifically linked to the glucose levels. At low glucose concentration (5 mM), the fluorescence intensity was very low (**Figure 4.4B**) and only few cells responded to glucose for the calcium signaling, whereas un-induced cells did not show any fluorescence (**Figure 4.4A**). The highly enhanced fluorescence of the cells in the presence of 23 mM glucose demonstrates increased cell membrane depolarization for the enhanced calcium flux leading to insulin exocytosis (**Figure 4.4C**). This demonstrates the functional characteristics of the isolated hHPCs that are planned to use for further study where the role of different surface conditions such as conducting and non-conducting nature of substrates without changing the surface morphology and crystallite phase of the TiO_2 .

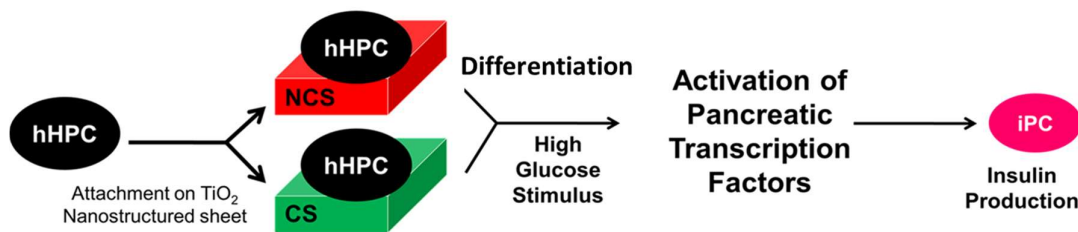


Figure 4.5: Schematic representation of developing conducting and non-conducting 3D-TiO₂ nanostructured sheets to support long-term cell survival and induced trans-differentiation of hHPCs into InPCs by activating Pdx-1 and β -cell transcription factor Nkx-6.1 in response to hyperglycemic challenge by providing extrinsic stimuli.

4.5 Differentiation of hHPCs into InPCs and relative gene analysis

4.5.1 Proposed strategy

The viability of cells during *in-vitro* culture stoutly depends on the surface chemistry and crystallite structure of the TiO₂ which has been reported in our earlier studies [77,87,97,118,120]. It has also demonstrated that hHPCs can be trans-differentiated into InPCs on collagen *in-vitro*, when stimulated by hyperglycemic challenge due to their common embryonic origin during the development of the pancreas [16,18]. However, as discussed in the introduction, this strategy had major drawbacks primarily owing to short-term cell survival and a low amount of insulin secretion. To address these points, the use of rutile TiO₂ of similar surface morphology on CS and NCS have any effect on *in vitro* differentiation of hHPCs into InPCs. Thus, a strategy for generating functional InPCs through differentiation of hHPCs under hyperglycemic condition in combination with the extrinsic stimuli of nanostructured TiO₂ supported with CS and NCS proposed and shown in schematic diagram **Figure 4.5**. This strategy was evolved to support the long-term cell survival and function. Further, to test the efficiency of hHPCs trans-differentiation into InPCs on CS and NCS, glucose was used as a stimulating factor. One million hHPCs (EpCAM+ve enriched) were

counted and seeded on collagen (referred as a control condition) coated surfaces and 5 mM to 30mM glucose was used to obtain the optimum glucose concentration needed for effective activation of pancreatic transcription factors. The investigation of glucose-challenged hHPCs indicates that these cells secrete a maximum level of insulin at 23 mM glucose after 24 h of stimulation (**Figure 4.3**).

4.5.2 Relative gene analysis for confirmation of activation of pancreatic transcription factors

The liver cells harvested from fetal tissues generally remain at various stages of the differentiation process, potentially generating hepatic, biliary and pancreatic lineages. Hence, we sought to characterize the developmental stages of trans-differentiating hHPCs on TiO₂ microchips after hyperglycemic (23 mM) stimulation *in vitro*. Total ribonucleic acid (RNA) was extracted from un-induced and 23 mM glucose-induced cells after day-1, day-3, and day-7 of incubation on three types of substrates using Trizol method (Invitrogen). Briefly, cells were harvested from the culture substrate using Trypsin-EDTA solution and cell pellet was obtained after centrifugation. The supernatant was discarded from each group of cells and 750µL of TRIzol™ Reagent was added to each vial of cells. The lysate was pipetted up and down several times to homogenize the cell pellet. 200 µL chloroform was added in each tube and incubated for 2–3 min at room temperature. Each sample was centrifuged for 15 min at 12,000 xg at 4°C. Transferred the aqueous phase containing the RNA to a new tube and added equal volume of ethanol in each tube to precipitate the RNA. Mixed and incubated the tube for 10 min at room temperature and centrifuged for 10 min at 12,000 xg at 4°C. Discarded the supernatant and air dried the RNA pellet for 5–10 min. Finally, resuspended the RNA pellet in 20–50 µL of RNase-free water with 0.1 mM EDTA. The extracted RNA was quantified and purity was calculated by nanodrop reading (Thermo scientific). Complementary de-oxy

ribonucleic acid (cDNA) was prepared from each group of RNA using Oligo dT primers (Invitrogen) and reverse transcriptase enzyme-II (Fermentas, Canada). Briefly, 12 μ L (100-1000 ng) of total isolated RNA was incubated with 2 μ L oligodT primer in a thermal cycler (Applied Biosystem) at 65°C for 10 min. Following to incubation, the reaction mixture was snap cooled in ice for 2 min and mixed with 8 μ L of 5X reverse transcriptase buffer, 1 μ L of 10 mM dNTPs mixture, and 0.5 μ L of 5 U/ μ L reverse transcriptase enzyme and 16.5 μ L of ddH₂O. This reaction mixture was further incubated at 42°C for 45-60 min followed by 10 min of extension at 72°C temperature. The integrity of prepared cDNA was confirmed by agarose gel electrophoresis with ethidium bromide staining under UV-trans-illuminator (BioRad). 5 ng cDNA was used for expression analysis of transcription factors (Pdx-1, Ngn-3, Isl-1, Pax-6, NeuroD1, Nkx-6.1, Pax-4, Nkx-2.2, and Glucagon) in each sample by using SYBR Green-based relative quantitation in StepOne RT-qPCR (Applied Biosystem, USA). A total of 20 μ L reaction mixture was prepared for analyzing each gene transcript in triplicate by adding 5 ng cDNA, 0.5 μ L of forward and reverse primers, 10 μ L of SYBR Green Mix (2X) and ddH₂O. The reaction was initially incubated at 95°C for 5 min denaturation, followed by 40 cycles of denaturation at 95°C for 40 sec, annealing at 50-60°C for 40 sec and extension at 72°C for 40 sec. The final extension was done at 72°C for 5 min and followed by 10 min melting curve analysis to distinguish between primer-dimer and amplicon. Glyceraldehyde 3-phosphate dehydrogenase (GAPDH) was used as an endogenous control for the normalization of the test samples. PCR efficiency was considered using $Y = mx + c$. The mean was taken for each sample and the fold difference was calculated using $2^{-\Delta\Delta CT}$ method by StepOne (Version 2.2) software in StepOne Real-Time PCR. R programming was used for statistical computing and graphical representation of fold difference values of different

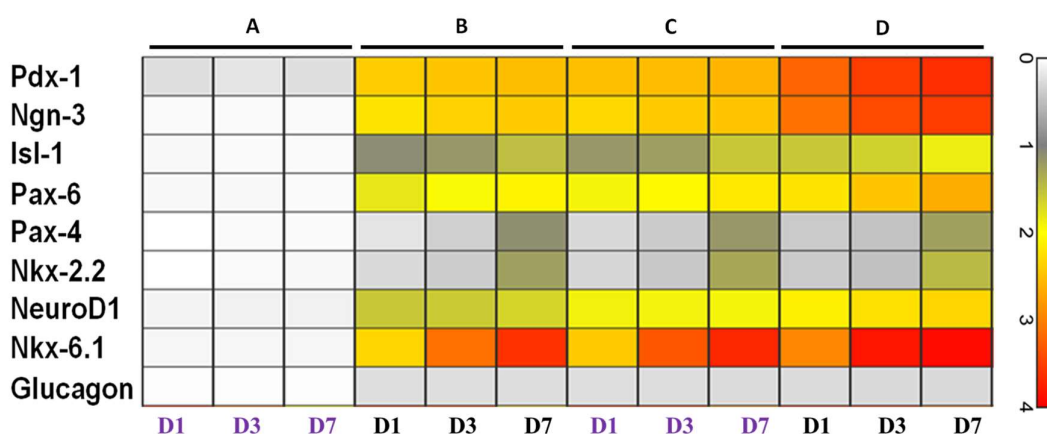


Figure 4.6: Heatmap of 15 mRNA transcripts including pancreatic and liver cell genes in un-induced (A) and 23 mM glucose-induced hHPCs after day 1, 3 and 7 cultured on collagen (B), NCS (C) and CS (D). Human pancreatic cells were used as positive control to compare the gene expression pattern with trans-differentiated cells in above three different conditions. At right side of heatmap the color bar represents the relative fold change in gene expression. Details of analysis are described in reference [120].

mRNA transcripts analyzed by RT-qPCR. The data were compiled and run on a UNIX platform during R programming (R Version 3.1.2). Interestingly, trans-differentiating hHPCs expressed master regulator Pdx-1, which generally triggers the activation of subsequent pancreatic transcription factors to induce the trans-differentiation of hHPCs into pancreatic cell lineages. The dynamic process of continuous alteration in the cell surface charge on hHPCs, grown on CS, in response to specific substrates and growth conditions (e.g., hyperglycemic growth media) can enforce activation of the pancreatic transcription factors (pTFs) that might enable higher yield of selective differentiation of hHPCs into InPCs. Further, to examine the comparative superiority of the nanostructured rutile TiO₂ microchips supported with CS and NCS nanostructures, we evaluated the expression of various pancreatic transcription factors (pTFs) by RT-qPCR analysis at different time points (0, 1, 3, and 7 days) in response to the hyperglycemic challenge to hHPCs cultured on TiO₂ nanostructures is shown in **Figure 4.6**. Three pancreatic β cell-specific TFs (Pdx-1, Nkx-6.1

and Pax-6), four transitional pancreatic markers (Ngn 3, Pax-4, Nkx-2.2, Isl1, and NeuroD1) and two pancreatic endocrine hormone markers (Insulin and glucagon) were quantified at mRNA level in hHPCs during trans-differentiation (Fig. 3). After 23 mM glucose stimulation, the transcript analysis revealed highly up-regulated (values in parenthesis shows relative fold increase) expression of Pdx-1 (3.21), Nkx-6.1 (2.94), Ngn-3 (3.11), Nkx-2.2 (0.42), Pax6 (2.21), Pax4 (.42), Isl1 (1.56), and NeuroD1 (2.12) at the end of 24 h on CS supported rutile-TiO₂ nanostructures as compared to 'day zero' i.e. un-induced cells. Importantly, hHPCs on the CS-supported rutile-TiO₂ showed consistently higher expression of the pTFs than cells in two other conditions (NCS supported TiO₂, or collagen 'control'). This finding demonstrates the commitment of majority of hHPCs towards the pancreatic endocrine precursor cells (specifically β -cells). Further, a gradual increase in the expression of pTFs at day 3 and day 7 cells suggests the proliferation and conversion of hHPCs into a higher population of InPCs on CS supported TiO₂ microchips *in vitro*. Among various pTFs, NKx-6.1 known to be responsible for the maintenance of differentiated state of β cells in the pancreas, was found to be significantly up-regulated in the microchips adhered cells (having expression level 2.94 on TiO₂ supported with CS and 2.42 on TiO₂ supported with NCS) as compared to the collagen-coated plastic surfaces. This finding suggests that most hHPCs are undergoing trans-differentiation quickly into functional InPCs. The higher expression of Isl1 (known to promote proliferation of islet cells) also suggests that proliferating hHPCs are more biased towards trans-differentiation into InPCs on the conducting surface (CS-TiO₂) than on NCS-TiO₂ and collagen surfaces after 24 h during hyperglycemic stimulation (23 mM).

4.6 Formation of three-dimensional pancreatic islet-like clusters

The glucose-stimulated hHPCs on CS-TiO₂ gradually formed three-dimensional pancreatic islet-like clusters, as shown in **Figure 4.7**, a phenomenon commonly observed during induced pancreatic β -cells differentiation from bone marrow hepatic and pancreatic stem cells [202,120]. Adherent cells on all three types of substrates induced with 23 mM glucose for 24 h (day 1), 72h (day 3) and 168 h (day 7) were harvested by trypsinization (using 0.25 % Trypsin-EDTA). The cells were co-stained with Pdx-1-PE with C-peptide-FITC and Nkx-6.1-PE with C-peptide as per the manufacturer's instructions.

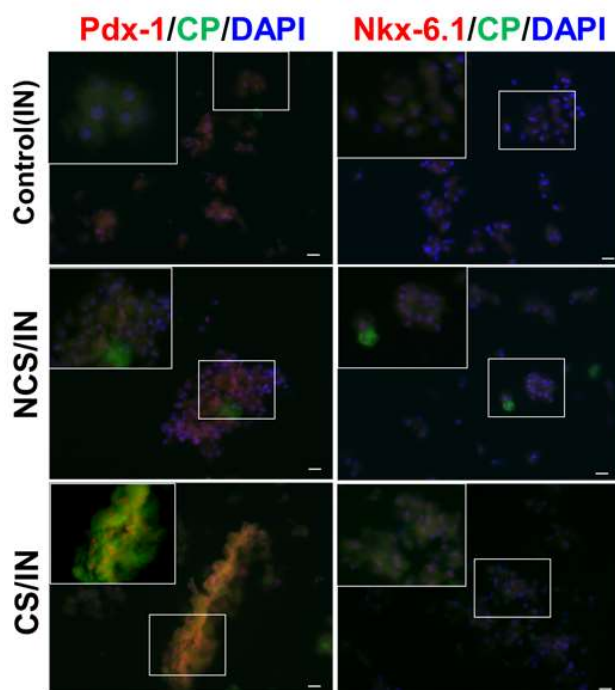


Figure 4.7: Trans-differentiated hHPCs after 24 h of 23 mM glucose stimulation express human β -cell specific markers. Representative immunocytochemistry of trans-differentiated hHPCs co-stained with nuclear protein Pdx-1 (red) with cytoplasmic protein C-peptide (green) and β -cell marker nuclear Nkx-6.1 (red) with cytoplasmic C-peptide (green). This observation revealed the enhanced co-expression of C-peptide with Pdx-1 and Nkx-6.1 respectively which shows the monohormonic nature of trans-differentiating cells responsible to produce higher amount of insulin on TiO₂ nanostructured implants specifically with CS. DAPI (blue) was used as counter staining of cellular nuclei in related groups. (Scale bar: 20 μ m).

Briefly, cells were fixed in 4 % PFA overnight at 4°C and treated with 1 % BSA solution to block the non-specific binding. After blocking cells were washed twice with 1X PBS and further incubated with respective secondary antibodies to stain the cell surface. For dual staining two-step staining protocol was followed. For intracellular staining cells were permeabilized with 0.1 % Triton-X-100 prior to staining. After staining, cells were washed three times with 1X PBS and mounted with DAPI mounting solution on microscopy slides. The immunofluorescence images of stained cells were documented by an inverted fluorescence microscope (Carl Zeiss, Germany).

Interestingly, trans-differentiated hHPCs on TiO₂ microchips seemed to contain a small population of glucagon-producing cells which was presumed after slight expression of glucagon mRNA. These cells (possibly α -cell type lineage) did not expand on the chips as indicated by the levels of the glucagon transcripts, which remained unchanged across the time points (1, 3, and 7 days). Altogether, the results suggest that EpCAM⁺ enriched hHPCs are more prone to trans-differentiate into pancreatic cell lineages during hyperglycemic stimulation, especially on rutile TiO₂-CS surface, which is a key factor found to achieve the highest functionality of human endocrine cells *in-vitro*.

To further confirm the trans-differentiation of hHPCs towards the pancreatic β -cell fate on CS-TiO₂ microchips under high glucose stimulation, we examined co-expression of the key markers at protein levels by immunofluorescence staining of Pdx-1 and Nkx-6.1 with C-peptide. The key β -cell transcription factors, Pdx-1 (the master regulator of pancreatic cell lineage) and Nkx-6.1 (responsible for β -cells maintenance in the pancreatic islets) were expressed at high levels after hyperglycemic stimulation. We also observed enhanced production of C-peptide (a stoichiometric byproduct of proinsulin processing) along with the co-expression of Pdx-1 and Nkx-6.1. This suggests that both trans-differentiation and insulin

production by hHPCs are tightly controlled by hyperglycemic stimulation (23 mM) in these cells (**Figure 4.7**). The co-expression of Pdx-1+/C-peptide+ cells adhered to TiO₂ nanostructures on NCS showed a higher percentage than in CS, which reveals that the majority of the cells population on NCS is still in transition to produce insulin where the activation of later cascade of pancreatic transcription factors is required which have already been activated in cells on CS. Similarly, the co-expression of C-peptide along with Nkx-6.1 was found to be highest in cells on TiO₂ nanostructures supported with CS. The co-expression of C-peptide along with Pdx-1 and Nkx-6.1 in InPCs on TiO₂-CS surface indicates that most cell populations represent monohormonic β -cell types that produce a higher amount of insulin, as depicted in **Figure 4.8**.

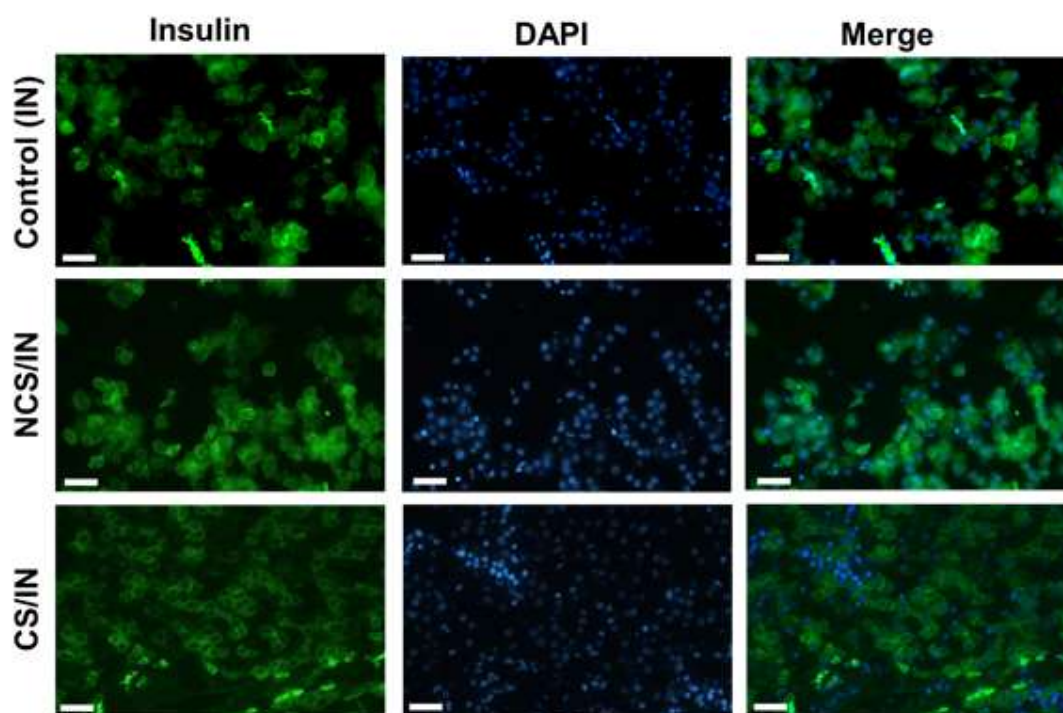


Figure 4.8: Immunocytochemical analysis of cytoplasmic insulin content in hHPCs during 23mM hyperglycemic challenge for 24 h on collagen-coated tissue culture plates (control), NCS and CS (scale bar 20 μ m). The amount of insulin produced inside the cells was represented with green fluorescence of anti-human insulin antibody, whereas the cell nuclei were counterstained with DAPI (in blue).

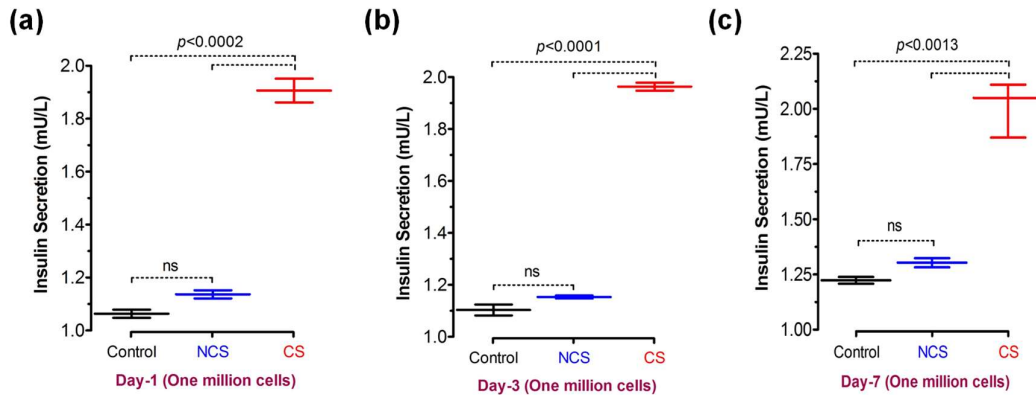


Figure 4.9: Whiskers plots showing the amount of insulin secreted from 23mM glucose-stimulated one million hHPCs cultured on collagen, NCS and CS after (a) day 1, (b) day 3 and (c) day 7 in culture media.

The immunofluorescence staining of cytoplasmic insulin content in the cells adherent on TiO₂-NCS and TiO₂-CS microchips showed the highest insulin content in the cells on TiO₂-CS compared to the other conditions. The remaining cell populations (unstained) were either pancreatic endocrine cells (α or δ cells which express hormones glucagon or somatostatin) or undifferentiated liver cells, which do not respond to glucose stimulus and express hepatic cell-specific mRNA transcripts.

4.7 Quantification of secreted insulin by differentiated hHPCs on TiO₂

Further, to confirm the active trans-differentiation of hHPCs into InPCs we examined the secretion of insulin in culture supernatant in above mentioned conditions. Insulin quantification in the culture media indicates that CS-TiO₂ adhered one million hHPCs after 24 h of hyperglycemic stimulation are more proficient (1.83 mU/L) than the control (collagen bound) or NCS-TiO₂ adhered cells (1.05 and 1.1 mU/L respectively) in secreting insulin and thus are more similar to the normal human pancreatic β -cells (1.75 mU/L) (Figure 4.9). The fact that these trans-differentiated cells can be maintained functionally equivalent to

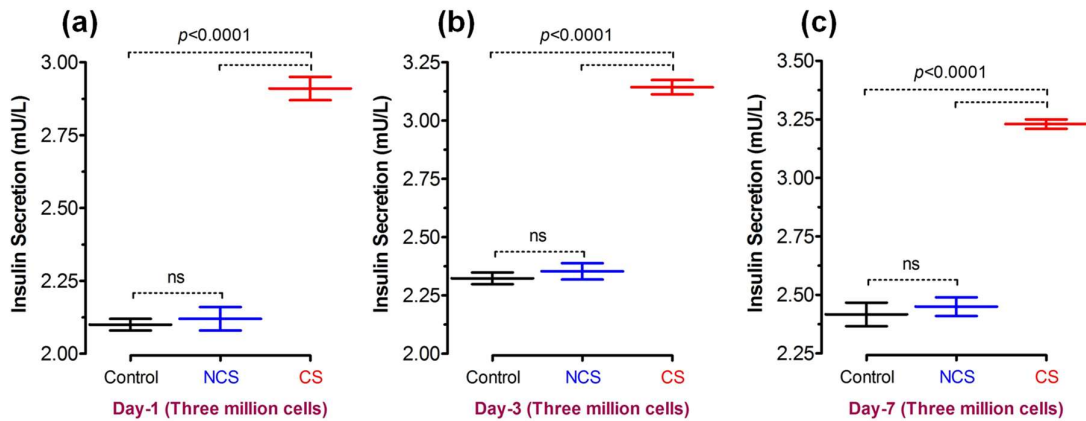


Figure 4.10: Whiskers plots showing the amount of insulin secreted from 23 mM glucose-stimulated three million hHPCs cultured on collagen, NCS and CS after (a) day 1, (b) day 3 and (c) day 7 in culture media.

pancreatic β -cells under a controlled hyperglycemic microenvironment suggest the superiority of CS-TiO₂ microchips for their therapeutic applicability. Further, it was examined the effects of cell number variation on insulin secretion by trans-differentiated hHPCs on TiO₂ microchips by culturing three (Figure 4.10), six (Figure 4.11), and nine million (Figure 4.12) cells on TiO₂-NCS and TiO₂-CS under hyperglycemic (23 mM) challenge for different time periods (1, 3, and 7 days). In all the conditions, the amount of insulin produced by the cells *in-vitro* was significantly higher in TiO₂-CS adherent hHPCs as compared to the cells on TiO₂-NCS and collagen (control group) at all time points. Although a larger number of cells produced enhanced insulin in all the conditions, however, the amount of secreted insulin was not exactly multiple of the arithmetic number of the adhered cells on the microchips. For example, one, three, six and nine million hHPCs secreted 1.03, 2.1, 2.9, and 3.6 mIU/L insulin when adhered to collagen (control) but produced 1.12, 2.08, 2.9, and 3.7 mIU/L from TiO₂-NCS chips, and 1.9, 2.9, 3.9, and 4.6 mIU/L from TiO₂-CS microchips following

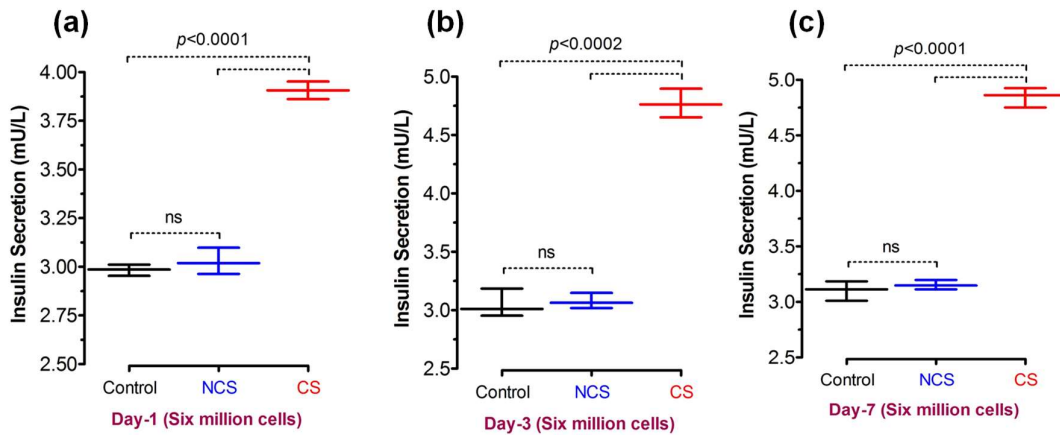


Figure 4.11: Whiskers plots of insulin secreted from 23mM glucose-stimulated six million hHPCs cultured on collagen, NCS and CS after (a) day 1, (b) day 3 and (c) day 7.

24 hrs of glucose-stimulated trans-differentiation (day 1). On day 7, the amount of insulin secreted by the trans-differentiating cells was found to increase respectively as follows: 1.2, 2.4, 3.1, and 3.7 mIU/L (control collagen surface), 1.3, 2.4, 3.1, and 3.8 mIU/L (TiO₂-NCS), and 1.9, 3.2, 4.85, and 4.95 mIU/L (TiO₂-CS). These data indicate that increasing the cell numbers from one to nine million per microchip enhances insulin production to the required level sufficient to control hyperglycemia in-vivo, approximately two folds at a given time point.

The insulin secretion by a given number of cells increases about three folds from day 1 to day 7 of glucose stimulation of hHPCs during *in-vitro* culture. The primary adult β -cells produce an average of 1.75 ± 0.25 mIU/L insulin, which was approximately similar to the amount of insulin produced by one million hHPCs during 24 h of trans-differentiation on TiO₂-CS microchips in response to 23 mM glucose stimulus.

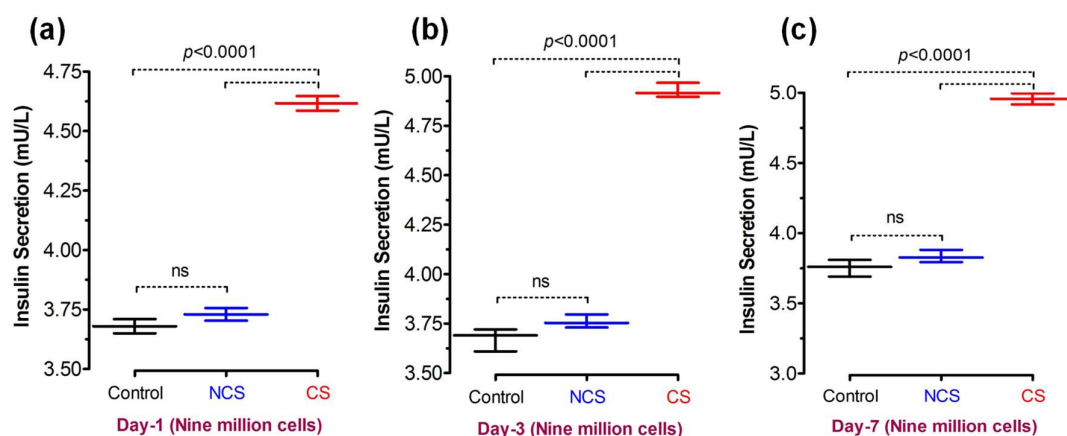


Figure 4.12: Whiskers plots showing the amount of insulin secreted from 23mM glucose-stimulated nine million hHPCs cultured on collagen, NCS and CS after (a) day 1, (b) day 3 and (c) day 7 in culture media.

We also examined the batch-to-batch variation of InPCs on TiO₂ microchips adhered trans-differentiated hHPCs during the hyperglycemic challenge (23 mM glucose) by immunofluorescence staining of the cells with insulin antibodies at different time points. Although slight variation was observed for insulin production during the hyperglycemic challenge from batch to batch, the overall reproducibility of InPCs was 81±10%.

4.8 STZ-induced hyperglycemia in C57BL6 mice and transplantation of InPCs on TiO₂

The potency of human InPCs on the rutile TiO₂-CS and TiO₂-NCS surface was tested for correcting hyperglycemia in a diabetic mouse, as shown in the schematic diagram in **Figure 4.13**. To investigate this, cellularised TiO₂-microchips were implanted in the peritoneal cavity of streptozotocin (STZ) induced diabetic C57BL6 male mice and identified their ability to restore normoglycemia. Animal study protocols were conducted after taking approval from the Institutional Animal Ethics Committee of Deccan College of Medical Sciences,

Hyderabad [120]. All the pre and post-operative care was supervised by the division of animal care staff. Animals were housed at $24^{\circ}\text{C}\pm 2^{\circ}\text{C}$ temperature, $55\%\pm 5\%$ humidity and at 12 h dark-light cycle. A standard rodent diet was given to all animals and allowed free access to food and water. Hyperglycemia was induced in C57BL6 mice (Gender: Male, Weight: 25-30gm, Age: 6-8week) using a low dose approach. 40mg/kg body weight streptozotocin (STZ) was administered intra-peritoneal for five consecutive days. Fasting blood glucose level was monitored every after 7 days of post-STZ injection.

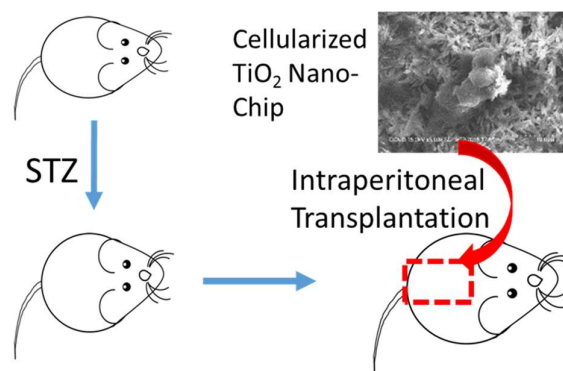


Figure 4.13: Schematic representation of cellularized TiO₂ nanostructured implants applicability at ectopic site in diabetic mice model [120].

To measure the blood glucose level of animals, clinically approved and commercial glucometer (GlucoChek, India) with range of 0-600 mg/dl was used. A small drop (2-4 μ l) of blood was collected from tail vein of mice using a lancet and blood glucose level was tested using disposable glucose measuring strips (GlucoChek, India). Mice with 6 h fasted glucose level below 150mg/dl were considered normoglycemic. In the study, the percentage morbidity of the diabetic groups of mice by scoring the survival of animals on every 10 days up to 90 days following transplantation was monitored and the results are shown in **Figure 4.14**.

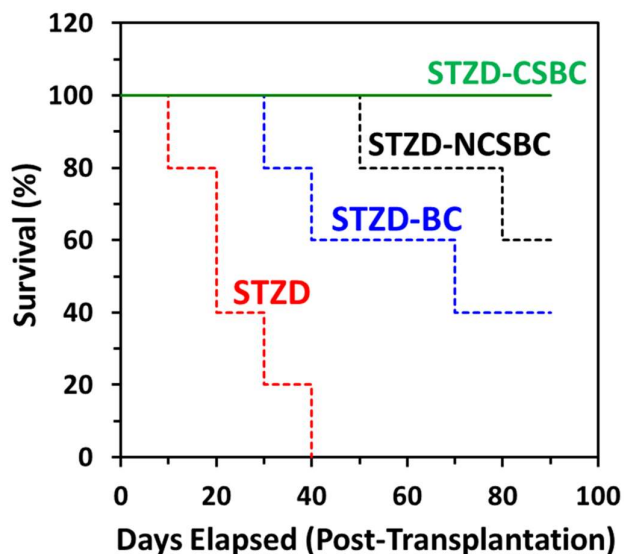


Figure 4.14: Kaplan Meier plot showing percentage of animals survived after STZ induced mice receiving saline (STZD), free trans-differentiated hHPCs implanted STZD (STZD-BC), trans-differentiated hHPCs on TiO_2 sheets prepared on NCS (STZD-NCSBC) and CS (STZD-CSBC).

Remarkably, all the mice which received InPCs- TiO_2 -CS implants showed 100% survival, while the other groups exhibited declined morbidity to different extents. The diabetic mice receiving InPCs- TiO_2 -NCS implants showed ~70% survival, and those with free InPCs only had 40% survival after 90 days post-transplantation.

Further, to demonstrate the usability of these chips for hyperglycemia control, blood glucose levels were monitored every after 10 days of post-transplantation in mice receiving the implant. Mice have fasted for 6 h before collection of the blood sample. Changes in blood glucose level were noted and compared with the diabetic and healthy mice at each time point up to 90 days post-transplantation. Before testing the blood glucose level, calibration of glucometer was checked. Strips were coded for each group of animals before testing. Each time, single strip was used for BGL testing. 2-10 μl of blood was drenched at the provided area on each strip after making a tiny prick in tail vein of the mice. Strip was inserted into the Blood Glucometer and displayed values were recorded.

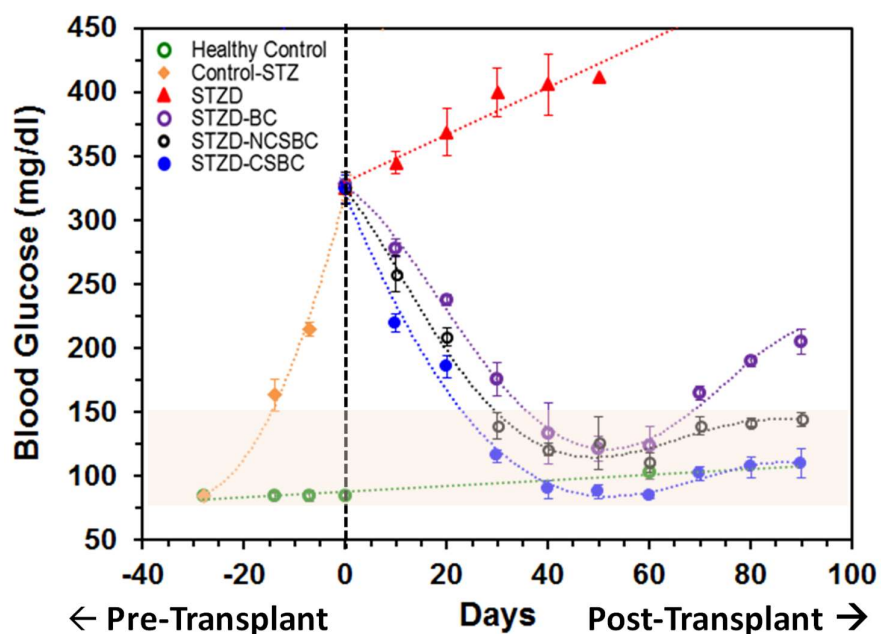


Figure 4.15: Fasting blood glucose level was monitored in healthy control and STZ-induced C57BL6 mice before (pre-implantation day 0-28, represented as day -28 to day 0) and after transplantation (post-implantation day 10-90 at every 10 days interval) of trans-differentiated free hHPCs, NSC-BC and CS-BC.)

STZ-treated diabetic mice were monitored for 28 days (pre-transplantation) to measure their blood glucose levels (BGL) which were higher than the normal level (≥ 300 mg/dl 6hrs fasting blood glucose), and TiO₂ implants were prepared by *in vitro* by transdifferentiation of hHPCs (1×10^6 cells) under 23 mM glucose stimulus for 24 h on TiO₂-CS and TiO₂-NCS microchips (ca. 10×10 mm²).

One set of diabetic mice received microchip transplants for further 90 days study (post-transplantation) that involved monitoring of blood glucose (Figure 4.15). The diabetic mice 'control' without the transplants showed progressively higher BGL (> 400 mg/dl), whereas those receiving InPCs-TiO₂ implants showed rapid normalization in their BGL (< 200 mg/dl at day 20). The infusion of free cells also showed BGL normalization, but amelioration was much slower (< 200 mg/dl at day 30) than those with the InPCs-TiO₂ implants. More

importantly, diabetic mice receiving InPCs-TiO₂-CS showed the fastest normoglycemia (200 mg/dl at day 20), which was steadily maintained up to 90 days. While both groups of diabetic mice that received InPCs on TiO₂ implants (prepared from CS and NCS) maintained their normal BGL, the group who received free InPCs showed a gradual increase (after 60 days) in their blood glucose that reached above 200 mg/dl at day ninety. These results demonstrate the superiority of InPC-cellularized TiO₂-microchips for remaining physiologically active at the ectopic site (peritoneal cavity) to ameliorate hyperglycemia faster and maintain long-term normoglycemia in animals.